Ethanol's action at BK channels accelerates the transition from moderate to excessive alcohol consumption

Agbonlahor Okhuarobo[1], Max Kreifeldt[1], Pushpita Bhattacharyya[1], Alex M Dopico[2], Amanda J Roberts[3], Gregg E Homanics[4], Candice Contet[1]*

Affiliations:

[1] The Scripps Research Institute, Department of Molecular Medicine, La Jolla, CA

[2] University of Tennessee Health Science Center, Department of Pharmacology, Addiction Science, and Toxicology, Memphis, TN

[3] The Scripps Research Institute, Animals Models Core Facility, La Jolla, CA

[4] University of Pittsburgh, Department of Anesthesiology and Perioperative Medicine, Pittsburgh, PA

*** Corresponding author**

Candice Contet

Address: The Scripps Research Institute, 10550 N Torrey Pines Road, SR-107, La Jolla, CA 92037, USA

Phone: 858 784 7209

Email: contet@scripps.edu

Short title: BK channels in alcohol dependence

Keywords: *Kcnma1*, Slo1, Maxi-K, knockin, vapor, inhalation, dependence, intermittent, abstinence

Abstract

Large conductance potassium (BK) channels are among the most sensitive molecular targets of ethanol. Whether the action of ethanol at BK channels influences the motivation to drink alcohol remains to be determined. In the present study, we sought to investigate the behavioral relevance of this interaction by introducing in the mouse genome a point mutation (BK α K361N) known to render BK channels insensitive to ethanol while preserving their physiological function. We demonstrate that preventing ethanol's interaction with BK channels at this site hinders the escalation of voluntary alcohol intake induced by repeated cycles of alcohol intoxication and withdrawal. In contrast, the mutation does not alter ethanol's acute behavioral effects, nor the metabolic and activity changes induced by chronic exposure to alcohol. Our findings point at BK channel ethanol-sensing capacity as a vulnerability mechanism in the transition from moderate alcohol consumption to pathological patterns of alcohol abuse.

Introduction

Calcium- and voltage-activated, large conductance potassium (BK) channels are one of the primary molecular targets of ethanol in the brain [1-3]. Depending on multiple molecular determinants (e.g., intracellular calcium concentration, alternative splicing, subunit composition, posttranslational modifications, lipid microenvironment), ethanol can either potentiate or reduce BK channel-mediated currents [reviewed in 4]. Whether the action of ethanol on mammalian BK channels mediates the behavioral effects of ethanol and influences the motivation to drink alcohol remains to be determined. Filling this gap of knowledge has critical implications for the understanding and treatment of alcohol use disorders (AUD) as it would support or put into question the potential of BK channels as a relevant therapeutic target in AUD.

Until now, the contribution of BK channels to the behavioral effects of ethanol has been studied by genetically manipulating the pore-forming α subunit in worms and flies, and the auxiliary β subunits in mice. Studies in invertebrates yielded disparate results, as BK α mediates the intoxicating effects of ethanol in worms [5, 6] while it mediates rapid tolerance to ethanol-induced sedation and increased seizure susceptibility in flies [7-11]. In mice, deletion of BK β4 promotes rapid tolerance to the locomotor depressant effect of ethanol [12] and attenuates ethanol drinking escalation in ethanol-dependent mice [13]. Conversely, deletion of BK β1 accelerates drinking escalation in dependent mice [13] and reduces chronic tolerance to ethanol-induced sedation and hypothermia [14]. These findings suggest that BK auxiliary subunits play a role in the adaptive response to chronic ethanol exposure in mammals but fail to provide a direct insight into the role of ethanol's interaction with BK pore-forming subunit in alcohol-related behaviors.

In the present study, we sought to establish whether the action of ethanol at BK channels contributes to excessive alcohol drinking in a mouse model of alcohol dependence. We first show the limitations of currently available pharmacological modulators of BK channels to

address this question and then turn to a genetic approach to block the interaction of ethanol with BK α without affecting basal BK channel function, by introducing a point mutation (K361N) known to selectively abolish BK channel activation by ethanol *in vitro* [15]. Our results demonstrate the key role of this BK channel ethanol-sensing site in the escalation of alcohol intake upon dependence induction. We further demonstrate that this role is not related to a differential sensitivity to ethanol's acute behavioral effects or to the metabolic and activity alterations induced by chronic exposure to ethanol. These findings provide tangible support for disabling the BK channel ethanol-sensing capacity as a strategy to hinder the transition from casual, moderate alcohol consumption to pathological patterns of alcohol abuse.

Materials and Methods

Animals

C57BL/6J mice were obtained from The Jackson Laboratory or from The Scripps Research Institute (TSRI) rodent breeding colony. BKα K361N knockin (KI) mice were generated at the University of Pittsburgh. Breeders were sent to TSRI, where a colony was maintained by mating heterozygous (Het) males and females such that experimental mice were littermates. KI males were backcrossed to C57BL/6J females every 1-2 years to prevent genetic drift.

Mice were maintained on a 12 h/12 h light/dark cycle. Food (Teklad LM-485, Envigo) and acidified or reverse osmosis purified water were available *ad libitum*. Sani-Chips (Envigo) were used for bedding substrate. All experiments were conducted in males and behavioral testing was started when they were at least 10 weeks old. Mice were single-housed for drinking experiments and group-housed otherwise. Testing was conducted during the dark phase of the circadian cycle, except for conditioned place preference, which was conducted during the light phase.

All procedures adhered to the National Institutes of Health Guide for the Care and Use of Laboratory Animals and were approved by the Institutional Animal Care and Use Committees of the University of Pittsburgh and TSRI.

Generation of BKα K361N KI mice

KI mice were produced using CRISPR/Cas9 technology as previously described in detail [16]. Briefly, a sgRNA targeting Kcnma1 in exon 9 near the intended mutation site was identified using the CRISPR Design Tool [17]. Two overlapping PCR primers (forward: GAAATTAATACG ACTCACTATAGGAGTGTCTCTAACTTCCTGAGTTTTAGAGCTAGAAATAGC; R: AAAAGCA CCGACTCGGTGCCACTTTTTCAAGTTGATAACGGACTAGCCTTATTTTAACTTGCTATTTCT AGCTCTAAAAC) were used to generate a T7 promoter containing sgRNA template as described (Bassett et al., 2014). The sgRNA and Cas9 mRNA were produced by *in vitro* translation, purified (MEGAclear Kit, Ambion), ethanol precipitated, and resuspended in DEPC treated water. A 120-nucleotide single stranded DNA repair template oligonucleotide harboring the desired mutations in exon 9 of *Kcnma1* was purchased as Ultramer DNA (Integrated DNA Technologies, Coralville, IA). sgRNA (25 ng/μl), Cas9 mRNA (50 ng/μl), and repair oligo (100 ng/μl) were combined and injected into the cytoplasm C57BL/6J one-cell embryos as described [18]. Embryos that survived injection were transferred to the oviduct of day 0.5 post-coitum pseudo-pregnant CD-1 recipient females. Pups resulting from injected embryos were screened for DNA sequence changes in exon 9 of the *Kcnma1* gene by PCR/DNA sequence analysis. A male founder mouse harboring the desired changes was mated to C57BL/6J females to establish the KI line. The *Kcnma1* exon 9 containing amplicon from all Het F1 animals that were shipped for the TSRI breeding colony were sequenced to verify the fidelity of the mutated locus. The founder mouse harbored no off-target mutations (data not shown) in any of the top 7 off-target sites predicted by the Off –Targets tool of the Cas9 Online Designer [19].

Mice were genotyped by subjecting tail clip lysates to polymerase chain reaction (PCR) using a pair of primers (forward: GCTTTGCCTCATGACCCTCT; reverse: TGAACAAGGGTGCTGCTTCA) that amplifies a 450-bp fragment of the *Kcnma1* gene. The PCR products were then digested with Tru1I and the resulting fragments were visualized by electrophoresis in an ethidium bromide-stained agarose gel. Tru1I digestion yielded two fragments (107 + 343 bp) in the wild-type (WT) allele and three fragments (107 + 149 + 194 bp) in the KI allele (see KI-specific Tru1I site in **Fig. 2A**).

To verify that the mutation was also present in *Kcnma1* mRNA, RNA was isolated from a KI mouse brain hemisphere using the RNeasy Plus Universal Mini Kit (Qiagen, 73404), 2 µg of RNA was reverse-transcribed using the Transcriptor First Strand cDNA Synthesis Kit with random hexamer primers (Roche, 04379012001), and a 370-bp fragment (nucleotides 1304-1673 of NM_010610.3) was amplified from the resulting cDNA. This fragment was cloned into pBluescript II and sequenced with a T3 primer (Genewiz).

Experimental cohorts

Independent cohorts of C57BL/6J males were used to test the effects of penitrem A on tremors (n=28), alcohol drinking (n=20) and saccharin drinking (n=20), as well as the effects of paxilline (n=18) and BMS-204352 (n=30) on alcohol drinking.

Body weights were measured in experimentally naïve mice at 6 weeks of age (WT, n=7; Het, n=12; KI, n=6). Three independent cohorts of mice, each containing an equivalent number of WT and KI mice, were tested for alcohol drinking and their data were pooled for analysis (WT, n=21; KI, n=17). Ethanol clearance rate was measured in another cohort (WT, n=3; Het, n=4; KI, n=4). Separate cohorts were tested for ethanol-induced ataxia, sedation, and hypothermia (WT, n=10; Het, n=11; KI, n=8), ethanol-induced analgesia (WT, n=7; Het, n=9; KI, n=7), and conditioned place preference (WT, n=11; KI, n=15). Two additional cohorts were used to

measure activity/metabolism (WT, n=8; KI, n=7) and circadian rhythmicity (WT, n=8; KI, n=8) during withdrawal from chronic intermittent ethanol (CIE) exposure.

Ethanol drinking

Mice were single-housed 3 days before testing started and remained single-housed throughout the duration of the experiment. Voluntary ethanol consumption was assessed in 2-h sessions during which mice had access to a bottle of water and a bottle of 15% (v:v) ethanol (two-bottle choice [2BC]) in their home cage. 2BC sessions started at the beginning of the dark phase (except for the penitrem A study, in which sessions were started 2 h into the dark phase) and were conducted Mon-Fri. The position of the ethanol and water bottles was alternated each day to control for side preference. Ethanol intake was determined by weighing bottles before and after the session, subtracting the weight lost in bottles placed in an empty cage (to control for spill/evaporation) and dividing by the mouse bodyweight (measured weekly). A similar procedure was used to assess saccharin (0.005% w:v) consumption in the penitrem A study.

Pharmacological modulation of BK channels

Penitrem A was purchased from Sigma (P3053) for tremor assessment and from Enzo Life Sciences (BML-KC157) for drinking experiments. It was dissolved in dimethylsulfoxide (DMSO) at 10 mg/mL and diluted in saline for intraperitoneal (i.p.) injection (0.1 mL per 10 g body weight). The final concentration of DMSO was 50% for the 0.2 and 0.5 mg/kg doses, and 10% for the 0.05 and 0.1 mg/kg doses. The effects of penitrem A on tremor, ethanol drinking, and saccharin drinking were tested in three independent cohorts. Tremors were scored according to the following scale [20]: 0 = no tremor; 1 = no resting tremor, short-lasting low-intensity shaking elicited by handling; 2 = no resting tremor, continuous low-intensity shaking elicited by handling; 3 = spontaneous low-intensity tremor, aggravated by handling; 4 = severe spontaneous tremor,

convulsive episode elicited by handling; score 5 was not observed. For drinking experiments, penitrem A was injected 30 min prior to 2BC session start.

Paxilline was purchased from Sigma (P2928), dissolved in DMSO at 10 mM and diluted in phosphate-buffered saline (137 mM NaCl, 2.7 mM KCl, 1.8 mM KH_2PO_4, 10.1 mM Na_2HPO_4, pH 7.4) for i.p. injection (1:2000 for 22 µg/kg dose, 1:400 for 110 µg/kg dose, 1:80 for 550 µg/kg dose). Each dose was tested on a different week. Doses were tested in ascending order, and vehicle and drug treatments were counterbalanced over two consecutive days for each dose. This dose range was selected based on pilot testing that indicated reduced mobility at 1.1 mg/kg and tremors at 4.4 mg/kg, which would have confounded drinking behavior, as well as on reported anticonvulsant properties of ultra-low-dose paxilline [21].

BMS-204352 was purchased from Sigma (SML1313), dissolved in DMSO at 16 mg/mL and diluted in Tween-80:saline at a 1:1:80 ratio for i.p. injection. A dose of 2 mg/kg was selected based on its ability to reverse behavioral abnormalities in *Fmr1* mutant mice [22, 23].

Ethanol drinking escalation

CIE vapor inhalation was used to induce dependence and increase voluntary ethanol drinking in 2BC sessions, as described in [13, 24]. Mice were first subjected to ten 2BC sessions (Mon-Fri) and each genotype was split into two groups of equivalent baseline ethanol intake. Weeks of CIE (or air) inhalation (4 x 16-h intoxication/8-h withdrawal, Mon-Fri) were then alternated with weeks of 2BC (Mon-Fri) for a total of 3-5 rounds.

The inhalation chambers were made of sealed plastic mouse cages (Allentown). An electronic metering pump (Iwaki EZB11D1-PC) dripped 95% ethanol into a flask placed on a warming tray at a temperature of 50°C. Drip rate was adjusted to achieve target blood ethanol concentrations (BECs) of 150-250 mg/dL. An air pump (Hakko HK-80L) conveyed vaporized ethanol from the flask to each individual chamber. The air flow was set at a rate of 15 L/min for each pair of chambers. Each chamber was diagonally divided by a mesh partition to provide single housing

for two mice. Mice were injected i.p. with ethanol (1.5 g/kg, PHARMCO-AAPER, 111000200) and pyrazole (68 mg/kg, Sigma-Aldrich, P56607) diluted in saline, in a volume of 0.1 mL/10 g body weight, before each 16-h ethanol vapor inhalation session. Blood was sampled from the caudal vein at the end of a 16-h intoxication session. The tip of the tail was nicked with a scalpel blade, blood was collected with a heparinized capillary tube and centrifuged at 13,000 g for 10 min. BECs were measured using a GM7 analyzer (Analox) or by gas chromatography and flame ionization detection (Agilent 7820A). On CIE weeks, control (Air) mice received pyrazole only.

Motor coordination and ethanol-induced ataxia

Motor coordination was evaluated using an AccuRotor rotarod (Accuscan Instruments) accelerating from 4 to 40 rpm over 300 s. Mice were positioned on the rotating rod and speed at fall (rpm) was recorded. For motor learning, mice were subjected to 5 trials per day (30-90 min apart) for 3 consecutive days. For ataxia testing, the rod was rotating at a constant speed of 8 rpm and the mice had to stay on the rod for at least 30 s to pass. Ataxia testing was conducted 4-5 days after the last training trial and all mice were able to pass the criterion. They were then i.p. injected with 1.5 g/kg ethanol (0.1 mL/10 g body weight) and tested approximately every 4 min until they were able to pass the criterion again. At this point, blood was collected from the retroorbital sinus and processed for BEC determination using a GM7 analyzer (Analox Instruments, London, UK).

Ethanol-induced sedation and hypothermia

Baseline body temperatures were first determined using a MicroTherma 2K thermometer (ThermoWorks) fitted with a rectal probe. Mice were then i.p. injected with 3.5 g/kg ethanol (0.2 mL/10 g body weight), which resulted in loss of righting reflex (i.e., sedation). Mice were placed on their back and the time at which each mouse regained its righting reflex was recorded. At this

point, retroorbital blood was sampled and BECs were determined using a GM7 analyzer. Body temperatures were again recorded 60 and 120 min after injection.

Ethanol-induced analgesia

A digital Randall-Selitto apparatus (Harvard Apparatus 76-0234) was used to measure mechanical nociceptive thresholds, as described in [25]. The mouse was habituated to enter a restrainer made of woven wire (stainless steel 304L 200 mesh, Shanghai YiKai) over the course of 3 days. On testing days, the mouse was gently introduced into the restrainer and the distal portion of the tail was positioned under the conic tip of the apparatus. The foot switch was then depressed to apply uniformly increasing pressure onto the tail until the first nociceptive response (struggling or squeaking) occurred. The force (in g) eliciting the nociceptive response was recorded. A cutoff force of 600 g was enforced to prevent tissue damage. The measure was repeated on the medial and proximal parts of the tail of the same mouse, with at least 30 seconds between each measure. The average of the three measures (distal, medial, proximal) was used as nociceptive value for that day. The analgesic effect of ethanol was tested over 4 consecutive days using a Latin square design. Testing was conducted 5 min after i.p. injection of 20% v:v ethanol (0, 1.5, 2 and 2.5 g/kg, 0.1-0.17 mL/10 g body weight).

Ethanol conditioned place preference

The apparatus was made of matte black acrylic and consisted of a 42 cm long x 21 cm wide x 31 cm high rectangular box (inner dimensions) with a removable central divider (ePlastics, San Diego). In one compartment, the floor was covered with coarse mesh (stainless steel 304L 10 mesh, Shanghai YiKai) and the walls were decorated with white discs (5-cm dot sticker, ChromaLabel). In the other compartment, the floor was smooth and the walls were uniformly black. Pre-conditioning, conditioning, and post-conditioning trials were conducted on consecutive days, 2 h into the light phase of the circadian cycle. During the pre-conditioning and

post-conditioning tests, mice had access to both compartments during 15 min and their motion was video-recorded by a ceiling-mounted camera connected to ANY-maze (Stoelting Co., Wood Dale, IL). During the conditioning trials, the mice were i.p. injected with saline or 2 g/kg ethanol (20% v:v, 0.13 mL/10 g body weight) and immediately confined to the compartment paired with this treatment during 30 min. A biased design was used to assign compartments to saline or ethanol for each mouse, i.e., ethanol was always assigned to the least favorite compartment (mesh floor for 6 WT and 9 KI mice, smooth floor for 5 WT and 6 KI mice). Treatments were alternated for a total of 8 conditioning trials (4 saline and 4 ethanol) and the order of treatment was counterbalanced within each genotype. Conditioned place preference was reflected by an increase in the time spent in the ethanol-paired compartment after *vs*. before conditioning.

Ethanol clearance rate

Mice were i.p. injected with 2 g/kg ethanol (20% v:v, 0.13 ml/10 g body weight). Tail vein blood was collected 30 min, 90 min and 180 min later and processed for BEC determination by gas chromatography and flame ionization detection.

Metabolism and sleep

Mice were exposed to CIE every other week, starting with a priming week at sub-intoxicating BECs (WT, 46.2 ± 3.4 mg/dL; KI, 46.0 ± 10.3 mg/dL), and followed by 4 weeks at intoxicating BECs (WT, 156.0 ± 9.6 mg/dL; KI, 127.4 ± 3.4 mg/dL). Body composition was analyzed by quantitative nuclear magnetic resonance (EchoMRI 3-in-1, EchoMRI LLC, Houston, TX) 72 h after the last vapor exposure. Mice were then immediately placed in metabolic cages (Comprehensive Laboratory Animal Monitoring System, Oxymax, Columbus Instruments, Columbus, OH), at the beginning of the dark phase. The following data were collected every 18 min for a total of 108 h: oxygen consumption (VO_2), carbon dioxide production (VCO_2), food intake, water intake, and locomotor activity. The respiratory exchange ratio (RER), calculated as

265 VCO_2/VO_2, provides an indicator of the substrate being metabolized, ranging from 0.7 when the
266 predominant fuel source is fat to 1 when the predominant fuel source is carbohydrate [26].
267 Locomotor activity counts (beam interruptions) were used by CLAMS-HC Sleep Detection
268 function to track sleeping bouts, as defined by 4 (or more) consecutive 10-sec epochs with 0
269 activity counts [27]. The first 12 hours (dark phase) were considered habituation and excluded
270 from analysis. The following 96 h were binned by 12-h light and dark phases and averaged
271 across the 4 days for statistical analysis.
272
273 ***Circadian rhythmicity***
274 Mice were exposed to CIE every other week for a total of 4 weeks (average BECs: WT, 132.2 ±
275 8.5 mg/dL; KI, 129.7 ± 9.3 mg/dL) and transferred to individual locomotor activity cages
276 (Photobeam Activity System-Home Cage, San Diego Instruments, San Diego, CA) 72 h after
277 the last vapor exposure. Mice were maintained on a 12 h/12 h light/dark cycle for 7 consecutive
278 days, then switched to constant darkness for an additional 11 days. Ambulation counts
279 represent consecutive beam breaks (8 x 4 beams in the 18.5” x 10” frame) and were collected in
280 1-h bins. Chi-square periodogram analysis was conducted in R (‘zeitgebr’ package,
281 https://github.com/rethomics/zeitgebr) to determine the circadian period length and relative
282 power during constant darkness [28, 29], using the last 240 hours of recording and a 6-min
283 resampling rate (see **Fig. 6B**).
284
285 ***Data analysis***
286 Data were analyzed in Statistica 13.3 (Tibco Software Inc., Palo Alto, CA). Distribution normality
287 was evaluated using a Shapiro-Wilk test and parametric/non-parametric tests were selected
288 accordingly for analysis of variance (ANOVA). Tests using *t* and *z* distributions were two-tailed.
289 Tremor scores were analyzed by Kruskal-Wallis ANOVA of the area under the curve. Saccharin
290 drinking was analyzed by Friedman ANOVA and pairwise comparisons were conducted using

Wilcoxon tests. Ethanol drinking was analyzed by repeated-measures (RM) ANOVA for pharmacological experiments, unpaired t-test for baseline intake in WT/KI mice, or two-way ANOVA with genotype (WT, KI) and vapor (Air, CIE) as between-subject variables (weekly averages). *Posthoc* tests and planned comparisons were conducted using Tukey's test. The effect of genotype on ataxia and sedation was analyzed by one-way ANOVA. Ethanol's clearance rate was analyzed by two-way RM-ANOVA, with time as within-subject variable and genotype as between-subject variable. The hypothermic, analgesic, and rewarding effects were also analyzed by two-way RM-ANOVA, with time, dose, or conditioning, respectively, as within-subject variable and genotype as between-subject variable. EchoMRI data, circadian period length and relative power were analyzed by two-way ANOVA (genotype, vapor). CLAMS data were analyzed by three-way RM-ANOVA, with phase as within-subject variable and genotype and vapor as between-subject variables. When there was a significant interaction between phase and vapor, two-way ANOVAs were further conducted for each phase. Data are expressed as mean ± s.e.m.

Results

Non-tremorgenic pharmacological modulation of BK channel activity does not alter voluntary ethanol consumption

We first sought to examine the contribution of BK channels to voluntary ethanol consumption and dependence-induced intake escalation using a pharmacological approach in C57BL/6J males. Since ethanol can activate neuronal BK channels, we hypothesized that blocking BK channels may interfere with the motivational properties of ethanol and increase (to overcome BK channel blockade) or decrease (if blockade is unsurmountable) ethanol drinking.

We first used penitrem A, a brain-penetrant fungal alkaloid that potently inhibits BK channels [30, 31]. Penitrem A induced tremors in a dose-dependent manner (**Fig. 1A**, main effect of dose: $H_{3,24}$=23.4, p<0.0001; *posthoc* tests: p<0.05 vehicle *vs* 0.2 mg/kg; p<0.001 vehicle *vs* 0.5 mg/kg), as reported previously [32]. The dose of 0.2 mg/kg abolished both ethanol (**Fig. 1B**, dose effect: $F_{3,57}$=65.5, p<0.0001; *posthoc* test, p=0.0002 vehicle *vs* 0.2 mg/kg penitrem A) and saccharin (**Fig. 1C**, dose effect: $X^2_{3,19}$ =36, p<0.0001; *posthoc* test, p=0.0001 vehicle *vs* 0.2 mg/kg penitrem A) drinking. The dose of 0.1 mg/kg reduced ethanol intake (p=0.004) without affecting saccharin intake (p=0.97). The lowest dose of 0.05 m/kg did not affect ethanol (p=0.95) or saccharin (p=0.68) intake (**Fig. 1B-C**). Based on our previous findings in BK β1 and β4 knockout (KO) mice [13], we reasoned that an effect of BK channel blockade may selectively emerge in dependent mice that exhibit higher levels of ethanol intake. Accordingly, mice were exposed to CIE to escalate their voluntary ethanol drinking (**Fig. 1B vs Fig. 1D**, effect of vapor: $F_{1,9}$=141.7, p<0.0001). Under these conditions, the two lowest doses of penitrem A did not alter ethanol intake (**Fig. 1D**, dose effect: $F_{2,16}$=0.7, p=0.52).

Tremorgenic mycotoxins can inhibit BK channels via different mechanisms and may therefore have a differential effect on ethanol-induced potentiation of BK-mediated currents. Notably, the association of β1 subunits reduces BK channel sensitivity to penitrem A by 10-fold, while it does not affect sensitivity to paxilline, a highly selective BK channel blocker [31, 33]. Since β1 subunits influence ethanol intake escalation in CIE-exposed mice [13], we next tested the effect of paxilline in both non-dependent (Air) and dependent (CIE) mice. We limited our analysis to non-tremorgenic doses (see *Methods* for dose range determination). Paxilline did not affect ethanol intake regardless of the alcohol dependence status (**Fig. 1E**, dose effect: $F_{3,48}$=1.0, p=0.42; vapor effect: $F_{1,16}$=11.0, p=0.004; dose x vapor interaction: $F_{3,48}$=0.27, p=0.85).

To further investigate the ability of BK channels to modulate ethanol intake, we tested the effect of a BK channel opener, BMS-204352. At 2 mg/kg, a dose that rescues several behavioral

deficits of *Fmr1* KO mice [22, 23], BMS-204532 did not impact moderate (Air) or excessive (CIE) ethanol drinking (**Fig. 1E**, treatment effect: $F_{1,28}$=0.1, p=0.73; vapor effect: $F_{1,28}$=28.5, p<0.0001; treatment x vapor interaction: $F_{1,28}$=0.6, p=0.45).

Generation and validation of BK α K361N knockin mice

The significance of pharmacological manipulations is inherently limited because they perturb the physiological activity of BK channels rather than selectively antagonizing the effect of ethanol at BK channels. We therefore turned to a genetic approach to probe the role of ethanol's action at BK channels in the motivation to consume alcohol. Bukiya and colleagues discovered that an asparagine substitution of residue K361 of the mouse BK α subunit abolishes ethanol's ability to increase BK channel steady-state activity without affecting unitary conductance, calcium sensitivity, and voltage sensitivity, thereby providing a unique opportunity to directly and selectively disrupt the effect of ethanol on BK channels [15].

Accordingly, we generated a knockin (KI) mouse expressing the K361N mutant instead of the wildtype (WT) BK α on a C57BL/6J background. A CRISPR/Cas9 strategy was used to introduce two nucleotide mutations in the *Kcnma1* gene: A G-to-T missense mutation modifying the triplet encoding K361 into an asparagine-coding triplet, and a silent G-to-T mutation introducing a Tru1I restriction site to facilitate mouse genotyping (**Fig. 2A**). KI mice were viable and all three genotypes (KI, Het, and WT) were obtained in Mendelian proportions. The presence of the mutations in the *Kcnma1* mRNA was verified by mouse brain cDNA sequencing (**Fig. 2B**). We conducted behavioral assessments to verify that the basal function of BK channels was preserved in KI mice, based on the known phenotype of mice missing BK α. Accordingly, while BK α KO mice displayed 15-20% smaller body weights than their WT counterparts at 4 and 8 weeks of age [34], we found no effect of the K/N361 genotype on body

363 weight at 6 weeks of age (**Fig. 2C**, $F_{2,22}$=0.4, p=0.70). Furthermore, while BK α KO mice
364 displayed major motor coordination deficits [34], BK α K361N KI mice acquired the accelerating
365 rotarod task at the same rate as their Het and WT counterparts (**Fig. 2D**, effect of trial:
366 $F_{14,336}$=37.2, p<0.0001; effect of genotype: $F_{2,24}$=0.8, p=0.48; trial x genotype interaction:
367 $F_{28,336}$=0.8, p=0.73).

368

369 ***The BK α K361N mutation hinders escalation of voluntary alcohol intake in the CIE-2BC***
370 ***model of dependence***

371 BK α WT and K361N KI mice were given access to voluntary alcohol consumption in limited-
372 access 2BC sessions (**Fig. 3A**). There was a trend for higher intake in KI mice during the first
373 week (t_{36}=-1.9, p=0.066) but the difference subsided by the second week (t_{36}=-1.0, p=0.33), with
374 the two genotypes stabilizing at similar levels. Mice were then exposed to weeks of CIE (or Air
375 only) to trigger voluntary intake escalation during intercalated weeks of 2BC drinking (**Fig. 3B**).
376 Average BECs in WT and KI mice were 189.6 ± 14.2 mg/dL and 192.9 ± 18.0 mg/dL,
377 respectively (t_{28}=-0.1, p=0.89). As expected, there was a significant week x vapor interaction
378 ($F_{4,136}$=4.1, p=0.0039), reflecting the escalation of voluntary alcohol consumption in CIE-
379 exposed mice. During the fourth postvapor week (PV4), planned comparisons detected a
380 significant difference between Air- and CIE-exposed WT mice (p=0.010), but not between Air-
381 and CIE-exposed KI mice (p=0.76), indicating that, by PV4, ethanol consumption had escalated
382 in WT but not KI mice. Furthermore, CIE-exposed WT mice consumed significantly more alcohol
383 than their KI counterparts (p=0.014), while there was no difference between Air-exposed WT
384 and KI mice (p=0.99). In conclusion, the BK α K361N mutation does not affect moderate alcohol
385 drinking but hinders the transition to excessive alcohol intake elicited by vapor exposure.

386

The BK α K361N mutation does not affect sensitivity to acute effects of alcohol

We sought to determine whether the reduced propensity of BK α K361N KI mice to escalate their alcohol consumption could be related to a differential sensitivity to some of the acute effects of alcohol. We first verified that there was no effect of genotype on the clearance rate of ethanol (effect of time: $F_{2,16}$=359.6, p<0.0001; effect of genotype: $F_{2,8}$=0.01, p=0.99; time x genotype interaction: $F_{4,16}$=0.2, p=0.91, **Fig. 4A**). In the rotarod assay, WT, Het, and KI mice were similarly sensitive to the loss of motor coordination induced by 1.5 g/kg ethanol; there was no effect of genotype on ataxia duration ($F_{2,26}$=1.0, p=0.37, **Fig. 4B**) and on BECs measured at recovery ($F_{2,26}$=2.0, p=0.16, **Fig. 4C**). Likewise, WT, Het and KI mice exhibited similar durations of loss-of-righting-reflex following administration of 3.5 g/kg ethanol ($F_{2,26}$=0.5, p=0.95, **Fig. 4D**) and similar BECs at recovery ($H_{2,26}$ =4.1, p=0.13, **Fig. 4E**). The amplitude of hypothermia was also identical across genotypes (effect of time: $F_{2,52}$=239.6, p<0.0001; effect of genotype: $F_{2,26}$=0.4, p=0.66; time x genotype interaction: $F_{4,52}$=0.5, p=0.71, **Fig. 4F**). Ethanol exerted a similar analgesic effects in WT, Het and KI mice at 1.5-2.5 g/kg doses (effect of dose: $F_{3,60}$=61.0, p<0.0001; effect of genotype: $F_{2,20}$=2.0, p=0.16; dose x genotype interaction: $F_{6,60}$=0.6, p=0.73, **Fig. 4G**). Finally, the rewarding effect of 2 g/kg ethanol was equivalent in WT and KI mice, as measured by conditioned place preference (effect of conditioning: $F_{1,24}$=25.6, p<0.0001; effect of genotype: $F_{1,24}$=0.6, p=0.43; conditioning x genotype interaction: $F_{1,24}$=0.04, p=0.85, **Fig. 4H**). Altogether, the BK α K361N mutation had no influence on the sensitivity of mice to multiple behavioral and physiological acute effects of moderate and high doses of ethanol.

Ethanol's action at BK channels does not mediate the effect of chronic alcohol exposure on metabolism, food intake, and locomotor activity

We then tested whether, in addition to their resistance to the motivational effect of CIE on alcohol drinking, KI mice might also be spared from physiological changes relevant to AUD, such as metabolic [35] and sleep [36] disturbances. EchoMRI analysis indicated that CIE significantly altered body composition (**Fig. 5A**), reducing fat content ($F_{1,10}$=9.8, p=0.011) while increasing lean content ($F_{1,10}$=10.6, p=0.0086), in the absence of body weight change ($F_{1,10}$=0.001, p=0.98, **Fig. 5B**). Metabolic monitoring also revealed increases in dark-phase food intake ($F_{1,10}$=7.3, p=0.023, **Fig. 5C**) and dark-phase RER ($F_{1,10}$=15.7, p=0.0027, **Fig. 5D**) in CIE-withdrawn mice. The K361N mutation did not influence any of these outcomes (F's<1.0, p's>0.34 for main effect of genotype and genotype x vapor interaction). Furthermore, neither genotype nor CIE affected sleep measures (**Fig. 5E-F, Table 1**).

Finally, given the role of BK channels in regulating neuronal excitability in the suprachiasmatic nucleus (the primary circadian pacemaker in mammals) [37, 38] and the desynchronization of biological rhythms observed in AUD [39, 40], we sought to determine whether the action of ethanol on BK channels could be responsible for a disruption of circadian rhythmicity in CIE-exposed mice. Under a standard light-dark cycle, the ambulation of CIE-exposed mice was significantly reduced up to withdrawal day 8 (vapor x time interaction: $F_{13,156}$=10.3, p<0.0001, see **Fig. 6A** for significance of vapor effect at individual timepoints). There was no significant influence of genotype on ambulation nor on the depressant effect of CIE withdrawal (genotype effect: $F_{1,12}$=0.5, p=0.49; genotype x vapor interaction: $F_{1,12}$=0.08, p=0.78). To test the function of the intrinsic pacemaker, mice were then switched to constant darkness for 10 days and chi-square periodogram analysis was used to determine the period length and relative power of the dominant circadian component of ambulation counts (**Fig. 6B-D**). Two-way ANOVA revealed a significant interaction between vapor and genotype on period length ($F_{1,12}$=6.5, p=0.025), but

none of the pairwise comparisons reached significance. Neither the K361N mutation nor alcohol withdrawal significantly affected the relative power (genotype effect: $F_{1,12}$=2.5, p=0.14; vapor effect: $F_{1,12}$=2.2, p=0.17; genotype x vapor interaction: $F_{1,12}$=0.60, p=0.45).

In conclusion, the lack of voluntary alcohol intake escalation observed in BK α K361N KI mice after 4 weeks of CIE exposure is not due to a differential sensitivity to the metabolic and locomotor effects of CIE withdrawal.

Discussion

Our data demonstrate that preventing ethanol from interacting with BK pore-forming subunit impedes the escalation of voluntary alcohol drinking in mice exposed to CIE, without altering the initiation or maintenance of alcohol drinking in control mice. Surprisingly, this manipulation did not affect the response of mice to acute ethanol or withdrawal from CIE, as evaluated in multiple behavioral and physiological assays. We also did not observe a consistent effect of BK channel pharmacological modulators administered acutely at non-tremorgenic doses on ethanol intake. Altogether, these findings support a critical role of ethanol's action at BK channels in the induction of neuroadaptations driving adverse motivational consequences of chronic alcohol exposure in mammals, which has relevance for AUD in humans.

The major behavioral disturbances elicited by the blockade of BK channels have historically been a hurdle to analyze the behavioral relevance of ethanol's action at this target. This limitation is illustrated by the results of our pharmacological experiments, whereby the dose-dependent effects of penitrem A on ethanol intake were impossible to disentangle from tremor induction. Paxilline injected at doses at least ten times lower than doses typically used to induce tremors (6-8 mg/kg, [33, 41]) did not cause overt behavioral abnormalities and marginally increased ethanol intake. An even lower dose of paxilline had been previously shown to reverse

459 picrotoxin- and pentylenetetrazole-induced seizures in the absence of tremors [21], which
460 suggest that the doses we used were high enough to significantly reach and block BK channels
461 in the mouse brain. On the other hand, BK channel activation by BMS-204352, at a dose known
462 to acutely reverse the sensory hypersensitivity and social interaction deficits of *Fmr1* KO mice
463 [22, 23], had no effect on ethanol intake. In our earlier work in BK β1 and BK β4 KO mice,
464 genotypic differences in ethanol intake only emerged after CIE exposure [13], suggesting that
465 CIE-exposed mice may be more sensitive to BK channel modulation. However, the effects of
466 penitrem A, paxilline, and BMS-204352 were qualitatively similar in Air- and CIE-exposed mice.
467 In conclusion, aside from tremors, acute pharmacological modulation of BK channels does not
468 interfere with alcohol drinking, which suggests that ethanol's interaction with BK channels is
469 unlikely to mediate the sensory, interoceptive, and reinforcing properties of this molecule.

470 To overcome the limitations of BK channel pharmacological modulation, we turned to a genetic
471 approach capitalizing on our current understanding of the structural determinants of ethanol's
472 action of BK channels, with K361 playing a key role as hydrogen bond donor in ethanol
473 recognition by the BK α cytoplasmic tail domain and the ensuing increase in channel open
474 probability [15]. Importantly, while the K361N substitution confers refractoriness to 100 mM
475 ethanol, it does not alter basal steady-state activity of BK channels, nor their sensitivity to the
476 BK channel primary endogenous activators: voltage and intracellular calcium [15]. This
477 selectivity is supported by our observation that K361N KI mice do not display reduced body
478 weights or motor learning deficits, as reduced BK channel function would be expected to
479 partially replicate the previously described phenotypes of BK α KO mice [34].

480 The K361N substitution did not alter levels of alcohol intake during acquisition, nor during
481 maintenance in Air-exposed mice. This finding is consistent with our earlier work in BK β1 and
482 BK β4 KO mice, which did not differ from their WT counterparts in several paradigms of
483 voluntary alcohol drinking unless they were also exposed to CIE [13]. Our data therefore

484 demonstrate that ethanol's action at BK channels is not necessary for alcohol to exert positive
485 reinforcing effects. On the other hand, alcohol intake escalation induced by CIE exposure was
486 blunted in K361N KI mice, indicating that ethanol's action at BK channels does contribute to
487 increasing the motivation to self-administer alcohol in mice that undergo repeated cycles of
488 alcohol intoxication and withdrawal. This finding is in accordance with the blunted escalation
489 displayed by BK β4 KO mice, in which ethanol's action at neuronal BK channel undergoes rapid
490 desensitization, as well as with the accelerated escalation displayed by BK β1 KO mice, in
491 which ethanol-induced potentiation of BK-mediated currents is expected to be enhanced [12,
492 13, 42]. Altogether, these data indicate that the action of ethanol on BK channels during CIE
493 promotes alcohol drinking escalation. Accordingly, we propose that molecular adaptations
494 resulting from chronic activation of BK channels by ethanol facilitate the progression to
495 dependence. Future studies will determine the nature of these molecular adaptations. Based on
496 the network of molecules known to physically interact with BK channels, a plethora of proteins,
497 including calcium channels and cytoskeletal elements, may be involved [43]. Furthermore, given
498 the ability of nuclear BK channels to influence nuclear calcium signaling, cAMP response
499 element-binding protein-dependent transcriptional activity may also be recruited [44, 45].

500 A low level of response to alcohol represents a strong risk factor for an individual's propensity to
501 develop an AUD [46]. We therefore hypothesized that the blunted escalation of K361N KI mice
502 might be linked to a reduced sensitivity to alcohol's acute behavioral and physiological effects.
503 However, we did not detect any effect of the K361N mutation, in the heterozygous or
504 homozygous state, on the responses to low (ataxia), moderate (analgesia, reward), or high
505 (sedation, hypothermia) doses of ethanol. Our data therefore indicate that ethanol's action at BK
506 channels does not mediate alcohol intoxication in mice and that reduced sensitivity does not
507 explain the reduced propensity of K361N mice to escalate their voluntary alcohol intake upon
508 CIE exposure.

509 This finding highlights a major species divergence with respect to the role of BK channels in the
510 behavioral effects of acute alcohol exposure. Most notably, mutating *C. elegans* SLO-1 (BK
511 channel ortholog) residue T381 (equivalent to human BK channel T352) into an isoleucine
512 abolishes ethanol-induced activation of the channel and confers resistance to behavioral signs
513 of intoxication, i.e. egg laying inhibition and reduced locomotion [6]. This indicates that, in
514 contrast to mice, BK channel *is* a critical mediator of alcohol intoxication in worms. However, BK
515 channels were already known to play a drastically different role in flies. In this organism,
516 increased expression of the *slo* gene, which encodes *D. melanogaster* BK channel pore-forming
517 subunit, represents a counter-adaptation responsible for the development of tolerance to
518 sedation, as well as withdrawal-associated hyperexcitability [8-11]. Such a role may also be at
519 play in mammals.

520 We hypothesized that, aside from alcohol drinking escalation, ethanol's action at BK channels
521 may mediate other physiological consequences of CIE exposure. We found that 4 weeks of CIE
522 significantly altered the body composition of mice, reducing fat content and increasing lean
523 content without affecting their total body mass. This observation is consistent with reports of
524 reduced body fat in chronic alcoholics, in the absence of body weight change and in proportion
525 to the level of alcohol consumption [47-50]. Studies in mice chronically fed an alcohol liquid diet
526 have indicated that chronic alcohol reduces white, rather than brown, adipose tissue and that
527 such lipolysis is associated with hepatic steatosis, i.e. ectopic deposition of fat in the liver [see
528 35 for review]. Interestingly, CIE-exposed rats and mice do not show evidence of hepatic
529 steatosis [51, 52]. The CIE procedure may therefore induce changes in lipid metabolism that
530 reflect an early stage of the development of alcohol liver disease. Multiple molecular
531 mechanisms have been proposed to underlie alcohol-induced lipolysis [reviewed in 35]; our data
532 indicate that chronic activation of BK channels by ethanol is not implicated.

The leaner phenotype of CIE-exposed mice was associated with a significant increase in food intake during the first week of withdrawal, which may reflect a homeostatic adaptation to the loss of body fat. In humans, chronic alcohol abuse increases daily caloric intake, yet alcohol represents a substantial fraction of this intake, such that energy intake provided only by food ingestion is typically lower than in healthy counterparts [47, 48, 53]. In one study, 14 days of abstinence normalized the nutritional status of the alcoholic subjects, but it is not known whether a compensatory increase in food intake may have occurred during their first week of abstinence [53]. Withdrawal from CIE was also associated with a robust increase in RER, reflecting preferential utilization of carbohydrates as a fuel. The dark-phase RER of CIE-exposed mice even approached the maximal theoretical value of 1 (i.e., carbohydrates used as sole substrate). This RER pattern may result from deficient lipid storage, as reflected by reduced body fat, and a corresponding inability to sustain normal levels of fatty acid oxidation. However, this observation contrasts with the lower respiratory quotient, higher lipid oxidation, and reduced carbohydrate oxidation reported in human alcoholics, which all normalize after three months of abstinence [47, 48, 53, 54]. To the best of our knowledge, the possibility that a rebound increase in respiratory quotient may occur during the first week of abstinence has not been explored in humans. In any case, the phenotype of KI mice indicates that the action of ethanol at BK channels is not responsible for the nutritional and metabolic changes associated with early withdrawal from chronic alcohol exposure.

Sleep disturbances are a hallmark of AUD disorders; insomnia is commonly experienced during abstinence and may contribute to relapse [36]. In mice, 4 weeks of CIE exposure combined with 2BC reduces the quantity and quality of slow-wave sleep 4 days into withdrawal [55]. In the present study, CIE did not affect sleep parameters recorded in the CLAMS chambers (bouts of inactivity > 40 s). It is possible that this methodology is not sensitive enough or that concomitant 2BC experience is critical to detect sleep alteration. AUD have also been associated with a

dysregulation of the circadian rhythm [40]. While CIE strongly reduced locomotor activity across both light and dark phases up to 8 days into withdrawal, it did not significantly affect free-running circadian period and amplitude. These observations extend similar findings from an earlier study in which C57BL/6J males had been exposed to 3 weeks of CIE [56]. These negative results precluded us from testing the role of BK channels in the effects of chronic alcohol exposure on sleep and circadian rhythm.

In conclusion, our data show that, in the mouse, ethanol's interaction with BK channels facilitates the escalation of voluntary alcohol intake produced by repeated cycles of alcohol intoxication and withdrawal. This role is dissociated from the metabolic and activity changes produced by chronic alcohol exposure and may instead contribute to increasing the motivational drive to consume alcohol. Furthermore, we demonstrate that BK channels do not mediate several acute behavioral effects of ethanol in mice, which contrast with previous findings obtained in *C. elegans*. By evolutionary extension, we propose that, in humans, BK channels may represent a valid target to counter allostatic adaptations associated with chronic alcohol exposure, rather than to block ethanol's acute effects. Future studies will aim to identify the brain regions and cellular populations in which BK channels may be gating molecular changes driving the transition to alcohol dependence.

Acknowledgments

We thank Dr. Elizabeth Thomas for lending us her rotarod apparatus, Dr. Mark Azar for his help with the tremor experiment, Brandon Hedges for his assistance with the paxilline experiment, and Carolyn Ferguson for expert technical assistance. We are also grateful for the support of TSRI's Animal Models Core, the Integrative Neuroscience Initiative on Alcoholism-Neuroimmune and the TSRI Alcohol Research Center Animal Models Core, which conducted blood ethanol concentration analysis for this study. This work was supported by the following grants from the National Institutes of Health: AA020913 (CC), AA006420 (CC, AJR), AA026685 (CC), AA027636 (CC), AA027372 (CC), AA020889 (GEH), AA10422 (GEH).

584 **Author contributions**

585 AO, MK, AJR, and CC performed behavioral experiments. AO, PB, AJR, and CC analyzed data.

586 CC and AJR designed experiments. GEH generated the knockin mice. AMD contributed to

587 conceptualization. CC conceived the study, acquired funds, and wrote the manuscript.

Disclosure

The authors declare no conflict of interest.

References

1. Dopico, A.M., Lemos, J.R., and Treistman, S.N. Ethanol increases the activity of large conductance, Ca(2+)-activated K+ channels in isolated neurohypophysial terminals. *Mol Pharmacol*, 1996. **49**(1): p. 40-8.
2. Martin, G., et al. Somatic localization of a specific large-conductance calcium-activated potassium channel subtype controls compartmentalized ethanol sensitivity in the nucleus accumbens. *J Neurosci*, 2004. **24**(29): p. 6563-72.
3. Abrahao, K.P., Chancey, J.H., Chan, C.S., and Lovinger, D.M. Ethanol-Sensitive Pacemaker Neurons in the Mouse External Globus Pallidus. *Neuropsychopharmacology*, 2017. **42**(5): p. 1070-1081.
4. Dopico, A.M., Bukiya, A.N., Kuntamallappanavar, G., and Liu, J. Modulation of BK Channels by Ethanol. *Int Rev Neurobiol*, 2016. **128**: p. 239-79.
5. Davies, A.G., et al. A central role of the BK potassium channel in behavioral responses to ethanol in C. elegans. *Cell*, 2003. **115**(6): p. 655-66.
6. Davis, S.J., Scott, L.L., Hu, K., and Pierce-Shimomura, J.T. Conserved single residue in the BK potassium channel required for activation by alcohol and intoxication in C. elegans. *J Neurosci*, 2014. **34**(29): p. 9562-73.
7. Cowmeadow, R.B., Krishnan, H.R., and Atkinson, N.S. The slowpoke gene is necessary for rapid ethanol tolerance in Drosophila. *Alcohol Clin Exp Res*, 2005. **29**(10): p. 1777-86.
8. Cowmeadow, R.B., et al. Ethanol tolerance caused by slowpoke induction in Drosophila. *Alcohol Clin Exp Res*, 2006. **30**(5): p. 745-53.
9. Ghezzi, A., Krishnan, H.R., and Atkinson, N.S. Susceptibility to ethanol withdrawal seizures is produced by BK channel gene expression. *Addict Biol*, 2014. **19**(3): p. 332-7.

614 10. Ghezzi, A., Pohl, J.B., Wang, Y., and Atkinson, N.S. BK channels play a counter-
615 adaptive role in drug tolerance and dependence. *Proc Natl Acad Sci U S A*, 2010.
616 **107**(37): p. 16360-5.
617 11. Ghezzi, A., Al-Hasan, Y.M., Larios, L.E., Bohm, R.A., and Atkinson, N.S. slo K(+)
618 channel gene regulation mediates rapid drug tolerance. *Proc Natl Acad Sci U S A*, 2004.
619 **101**(49): p. 17276-81.
620 12. Martin, G.E., et al. Identification of a BK channel auxiliary protein controlling molecular
621 and behavioral tolerance to alcohol. *Proc Natl Acad Sci U S A*, 2008. **105**(45): p. 17543-
622 8.
623 13. Kreifeldt, M., Le, D., Treistman, S.N., Koob, G.F., and Contet, C. BK channel beta1 and
624 beta4 auxiliary subunits exert opposite influences on escalated ethanol drinking in
625 dependent mice. *Front Integr Neurosci*, 2013. **7**: p. 105.
626 14. Kreifeldt, M., Cates-Gatto, C., Roberts, A.J., and Contet, C. BK Channel beta1 Subunit
627 Contributes to Behavioral Adaptations Elicited by Chronic Intermittent Ethanol Exposure.
628 *Alcohol Clin Exp Res*, 2015. **39**(12): p. 2394-402.
629 15. Bukiya, A.N., et al. An alcohol-sensing site in the calcium- and voltage-gated, large
630 conductance potassium (BK) channel. *Proc Natl Acad Sci U S A*, 2014. **111**(25): p.
631 9313-8.
632 16. Blednov, Y.A., et al. Mutation of the inhibitory ethanol site in GABAA rho1 receptors
633 promotes tolerance to ethanol-induced motor incoordination. *Neuropharmacology*, 2017.
634 **123**: p. 201-209.
635 17. Hsu, P.D., et al. DNA targeting specificity of RNA-guided Cas9 nucleases. *Nat*
636 *Biotechnol*, 2013. **31**(9): p. 827-32.
637 18. Yang, H., Wang, H., and Jaenisch, R. Generating genetically modified mice using
638 CRISPR/Cas-mediated genome engineering. *Nat Protoc*, 2014. **9**(8): p. 1956-68.

19. Guo, D., et al. Online High-throughput Mutagenesis Designer Using Scoring Matrix of Sequence-specific Endonucleases. *J Integr Bioinform*, 2015. **12**(1): p. 35-48.

20. Gallagher, R.T. and Hawkes, A.D. The potent tremorgenic neurotoxins lolitrem B and aflatrem: a comparison of the tremor response in mice. *Experientia*, 1986. **42**(7): p. 823-5.

21. Sheehan, J.J., Benedetti, B.L., and Barth, A.L. Anticonvulsant effects of the BK-channel antagonist paxilline. *Epilepsia*, 2009. **50**(4): p. 711-20.

22. Zhang, Y., et al. Dendritic channelopathies contribute to neocortical and sensory hyperexcitability in Fmr1(-/y) mice. *Nat Neurosci*, 2014. **17**(12): p. 1701-9.

23. Hebert, B., et al. Rescue of fragile X syndrome phenotypes in Fmr1 KO mice by a BKCa channel opener molecule. *Orphanet J Rare Dis*, 2014. **9**: p. 124.

24. Becker, H.C. and Lopez, M.F. Increased ethanol drinking after repeated chronic ethanol exposure and withdrawal experience in C57BL/6 mice. *Alcohol Clin Exp Res*, 2004. **28**(12): p. 1829-38.

25. Elhabazi, K., Ayachi, S., Ilien, B., and Simonin, F. Assessment of morphine-induced hyperalgesia and analgesic tolerance in mice using thermal and mechanical nociceptive modalities. *J Vis Exp*, 2014(89): p. e51264.

26. McLean, J.A. and Tobin, G. Animal and Human Calorimetry. 1987, Cambridge: Cambridge University Press. 338.

27. Pack, A.I., et al. Novel method for high-throughput phenotyping of sleep in mice. *Physiol Genomics*, 2007. **28**(2): p. 232-8.

28. Enright, J.T. The search for rhythmicity in biological time-series. *J Theor Biol*, 1965. **8**(3): p. 426-68.

29. Refinetti, R. Laboratory instrumentation and computing: comparison of six methods for the determination of the period of circadian rhythms. *Physiol Behav*, 1993. **54**(5): p. 869-75.

30. Knaus, H.G., et al. Tremorgenic indole alkaloids potently inhibit smooth muscle high-conductance calcium-activated potassium channels. *Biochemistry*, 1994. **33**(19): p. 5819-28.

31. Asano, S., et al. Penitrem A as a tool for understanding the role of large conductance Ca(2+)/voltage-sensitive K(+) channels in vascular function. *J Pharmacol Exp Ther*, 2012. **342**(2): p. 453-60.

32. Jortner, B.S., Ehrich, M., Katherman, A.E., Huckle, W.R., and Carter, M.E. Effects of prolonged tremor due to penitrem A in mice. *Drug Chem Toxicol*, 1986. **9**(2): p. 101-16.

33. Imlach, W.L., et al. The molecular mechanism of "ryegrass staggers," a neurological disorder of K+ channels. *J Pharmacol Exp Ther*, 2008. **327**(3): p. 657-64.

34. Sausbier, M., et al. Cerebellar ataxia and Purkinje cell dysfunction caused by Ca2+-activated K+ channel deficiency. *Proc Natl Acad Sci U S A*, 2004. **101**(25): p. 9474-8.

35. Steiner, J.L. and Lang, C.H. Alcohol, Adipose Tissue and Lipid Dysregulation. *Biomolecules*, 2017. **7**(1).

36. Chakravorty, S., Chaudhary, N.S., and Brower, K.J. Alcohol Dependence and Its Relationship With Insomnia and Other Sleep Disorders. *Alcohol Clin Exp Res*, 2016. **40**(11): p. 2271-2282.

37. Meredith, A.L., et al. BK calcium-activated potassium channels regulate circadian behavioral rhythms and pacemaker output. *Nat Neurosci*, 2006. **9**(8): p. 1041-9.

38. Harvey, J.R.M., Plante, A.E., and Meredith, A.L. Ion Channels Controlling Circadian Rhythms in Suprachiasmatic Nucleus Excitability. *Physiol Rev*, 2020. **100**(4): p. 1415-1454.

39. Lindberg, D., Andres-Beck, L., Jia, Y.F., Kang, S., and Choi, D.S. Purinergic Signaling in Neuron-Astrocyte Interactions, Circadian Rhythms, and Alcohol Use Disorder. *Front Physiol*, 2018. **9**: p. 9.

690 40. Meyrel, M., Rolland, B., and Geoffroy, P.A. Alterations in circadian rhythms following
691 alcohol use: A systematic review. *Prog Neuropsychopharmacol Biol Psychiatry*, 2020.
692 **99**: p. 109831.
693 41. Combs, M.D., Hamlin, A., and Quinn, J.C. A single exposure to the tremorgenic
694 mycotoxin lolitrem B inhibits voluntary motor activity and spatial orientation but not
695 spatial learning or memory in mice. *Toxicon*, 2019. **168**: p. 58-66.
696 42. Kuntamallappanavar, G. and Dopico, A.M. Alcohol modulation of BK channel gating
697 depends on beta subunit composition. *J Gen Physiol*, 2016. **148**(5): p. 419-440.
698 43. Kim, H. and Oh, K.H. Protein Network Interacting with BK Channels. *Int Rev Neurobiol*,
699 2016. **128**: p. 127-61.
700 44. Bengtson, C.P. and Bading, H. Nuclear calcium signaling. *Adv Exp Med Biol*, 2012. **970**:
701 p. 377-405.
702 45. Li, B., et al. Nuclear BK channels regulate gene expression via the control of nuclear
703 calcium signaling. *Nat Neurosci*, 2014. **17**(8): p. 1055-63.
704 46. Schuckit, M.A. Low level of response to alcohol as a predictor of future alcoholism. *Am J*
705 *Psychiatry*, 1994. **151**(2): p. 184-9.
706 47. Addolorato, G., Capristo, E., Greco, A.V., Stefanini, G.F., and Gasbarrini, G. Energy
707 expenditure, substrate oxidation, and body composition in subjects with chronic
708 alcoholism: new findings from metabolic assessment. *Alcohol Clin Exp Res*, 1997. **21**(6):
709 p. 962-7.
710 48. Addolorato, G., Capristo, E., Greco, A.V., Stefanini, G.F., and Gasbarrini, G. Influence of
711 chronic alcohol abuse on body weight and energy metabolism: is excess ethanol
712 consumption a risk factor for obesity or malnutrition? *J Intern Med*, 1998. **244**(5): p. 387-
713 95.

714 49. Addolorato, G., et al. Body composition changes induced by chronic ethanol abuse:
715 evaluation by dual energy X-ray absorptiometry. *Am J Gastroenterol*, 2000. **95**(9): p.
716 2323-7.
717 50. Liangpunsakul, S., Crabb, D.W., and Qi, R. Relationship among alcohol intake, body fat,
718 and physical activity: a population-based study. *Ann Epidemiol*, 2010. **20**(9): p. 670-5.
719 51. Mouton, A.J., et al. Alcohol Vapor Inhalation as a Model of Alcohol-Induced Organ
720 Disease. *Alcohol Clin Exp Res*, 2016. **40**(8): p. 1671-8.
721 52. Xu, J., et al. Blockade of IL-17 signaling reverses alcohol-induced liver injury and
722 excessive alcohol drinking in mice. *JCI Insight*, 2020. **5**(3).
723 53. Levine, J.A., Harris, M.M., and Morgan, M.Y. Energy expenditure in chronic alcohol
724 abuse. *Eur J Clin Invest*, 2000. **30**(9): p. 779-86.
725 54. Addolorato, G., et al. Three months of abstinence from alcohol normalizes energy
726 expenditure and substrate oxidation in alcoholics: a longitudinal study. *Am J*
727 *Gastroenterol*, 1998. **93**(12): p. 2476-81.
728 55. Huitron-Resendiz, S., et al. Effects of Withdrawal from Chronic Intermittent Ethanol
729 Exposure on Sleep Characteristics of Female and Male Mice. *Alcohol Clin Exp Res*,
730 2018. **42**(3): p. 540-550.
731 56. Logan, R.W., McCulley, W.D., 3rd, Seggio, J.A., and Rosenwasser, A.M. Effects of
732 withdrawal from chronic intermittent ethanol vapor on the level and circadian periodicity
733 of running-wheel activity in C57BL/6J and C3H/HeJ mice. *Alcohol Clin Exp Res*, 2012.
734 **36**(3): p. 467-76.

735

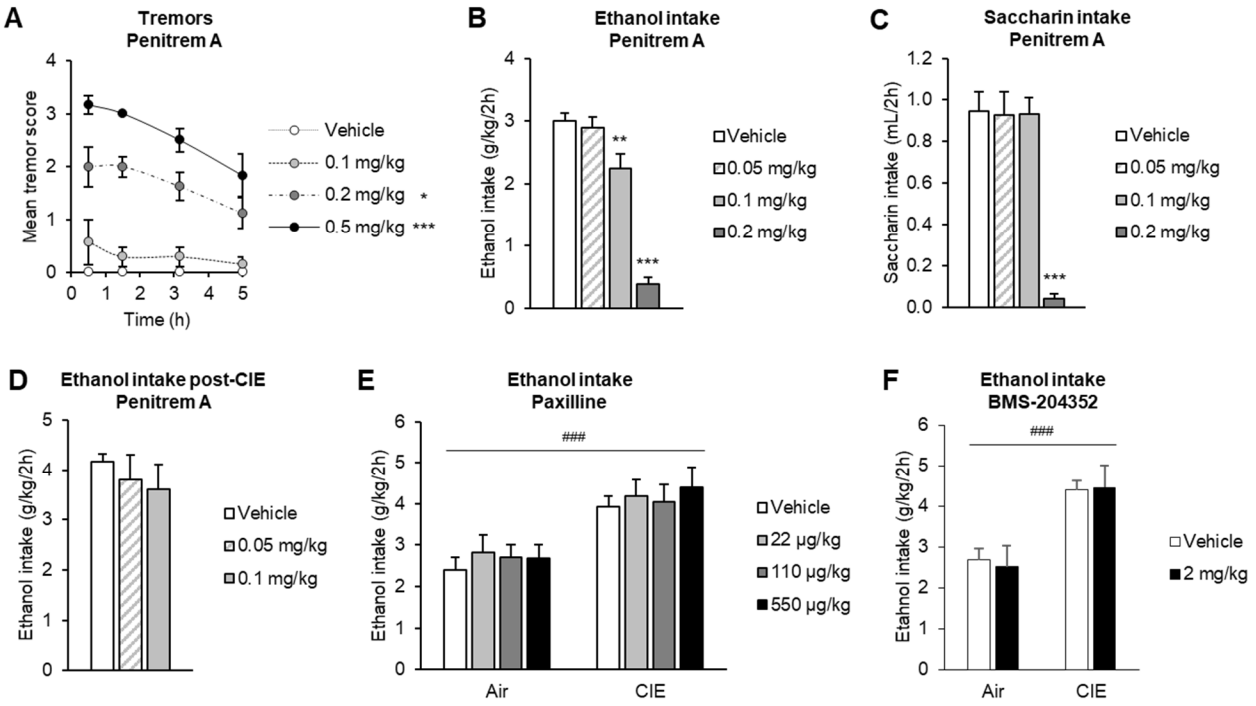

Figure 1. Low-dose pharmacological inhibition or activation of BK channels does not consistently alter alcohol drinking. A. Penitrem A, a BK channel blocker, induced tremors in a dose-dependent manner in alcohol-naïve C57BL/6J males (n=28, between-subject design). **B-F.** C57BL/6J male mice were given access to voluntary alcohol (**B, D-F**) or saccharin (**C**) consumption in 2-h two-bottle choice sessions. Some mice were exposed to chronic intermittent ethanol (CIE) vapor inhalation to induce dependence and increase voluntary ethanol intake, compared to mice inhaling air only (Air). **B-D.** Penitrem A reduced alcohol (B, n=20, within-subject design) and saccharin (C, n=20, within-subject design) intake at doses inducing tremors. CIE exposure did not sensitize mice to the effect of penitrem A (D, n=20, same mice as in B, within-subject design). **E.** Paxilline, a BK channel blocker, did not affect alcohol intake, across a range of non-tremorgenic doses and regardless of the dependence status of mice (n=18). **F.** BMS-204352, a BK channel opener, did not affect alcohol intake in Air or CIE mice (n=30). Significant difference with vehicle: *, $p<0.05$; **, $p<0.01$; ***, $p<0.001$. Significant main effect of CIE: ###, $p<0.001$. Data are shown as mean ± s.e.m.

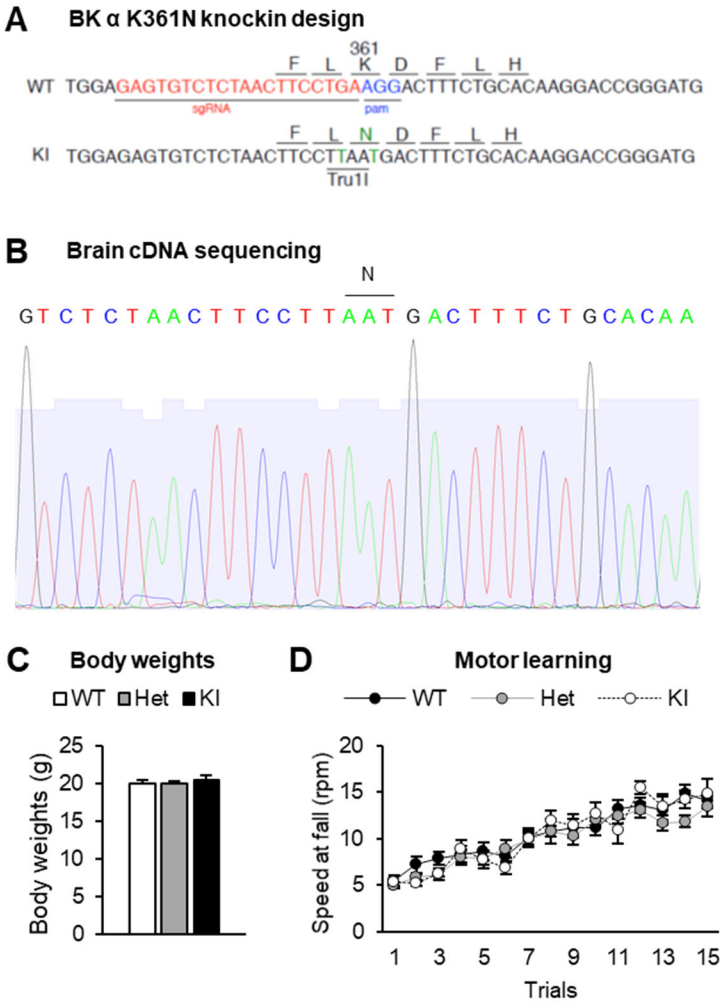

Figure 2. Generation of BK α K361N knockin (KI) mice. A. Design of the CRISPR/Cas9 construct used to introduce the K361N mutation in C57BL/6J mice. The single guide RNA (sgRNA) sequence is shown in red, the protospacer adjacent motif (PAM) is shown in blue, and the two mutated nucleotides are shown in green. WT, wildtype allele; KI, knockin allele. **B.** Verification of the mutated sequence in cDNA prepared from the brain of a K361N KI mouse. The triplet encoding the K361N mutation is highlighted. **C.** Body weights measured in males at 6 weeks of age (WT, n=7; Het, n=12; KI, n=6). **D.** Motor coordination measured in the accelerating rotarod assay in adult males (WT, n=10; Het, n=11; KI, n=8). There was no effect of genotype on either measure. Data are shown as mean ± s.e.m.

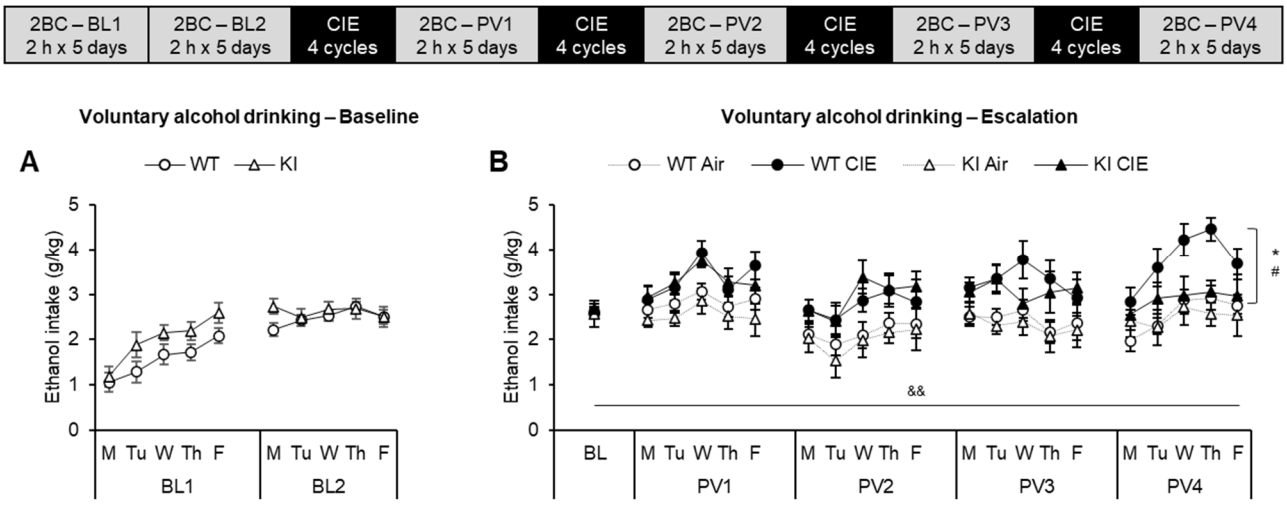

Figure 3. The BK α K361N mutation hinders alcohol drinking escalation in the CIE-2BC model of dependence. A-B. BK α K361N WT (n=21) and KI (n=17) mice were given access to voluntary alcohol consumption in 2-h two-bottle choice sessions prior to (**A**, and BL, baseline, in **B**) and in-between weeks of chronic intermittent ethanol (CIE) vapor inhalation (**B**). Statistical analysis was conducted on weekly averages. There was a significant week x vapor interaction ($^{\&\&}$, $p<0.01$). During PV4, CIE-exposed WT mice (n=10) consumed significantly more alcohol than their Air-exposed counterparts (n=11, p=0.010, $^{\#}$) and than CIE-exposed KI mice (n=9, p=0.014, *). In contrast, there was no difference between Air (n=8) and CIE-exposed KI mice (p=0.76). Data are shown as mean ± s.e.m.

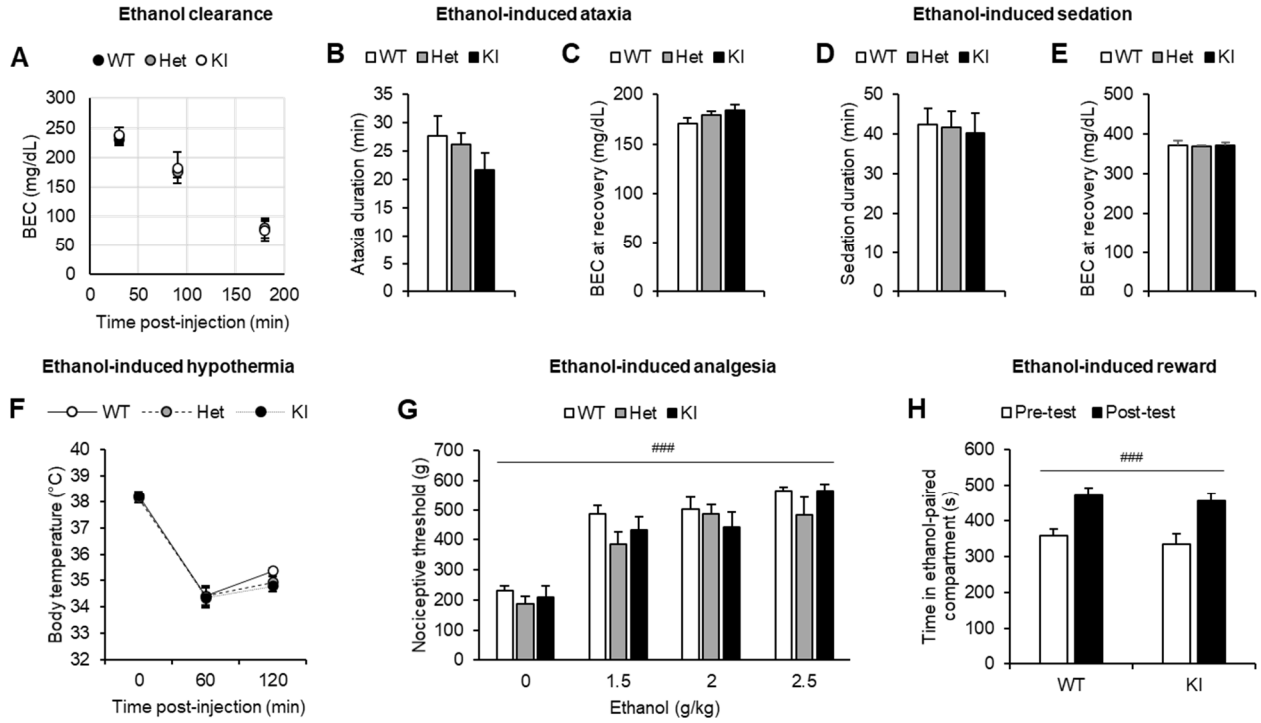

771

772 **Figure 4. The BK α K361N mutation does not affect sensitivity to acute effects of alcohol**

773 Measures of alcohol metabolism and intoxication were obtained in BK α K361N WT, Het and KI
774 mice acutely exposed to ethanol (i.p.). **A.** Blood ethanol concentration (BEC) clearance time-
775 course. **B-H.** Ethanol-induced ataxia (**B-C**, fixed-speed rotarod), sedation (**D-E**, loss of righting
776 reflex), hypothermia (**F**), analgesia (**G**, tail pressure test) and reward (**H**, conditioned place
777 preference). ###, effect of ethanol, $p<0.001$. None of the measures was significantly affected by
778 genotype. Sample sizes were as follows: **A:** WT, n=3; Het, n=4; KI, n=4. **B-F**: WT, n=10; Het,
779 n=11; KI, n=8. **G**: WT, n=7; Het, n=9; KI, n=7. **H**: WT, n=11; KI, n=15. Data are shown as mean
780 ± s.e.m.

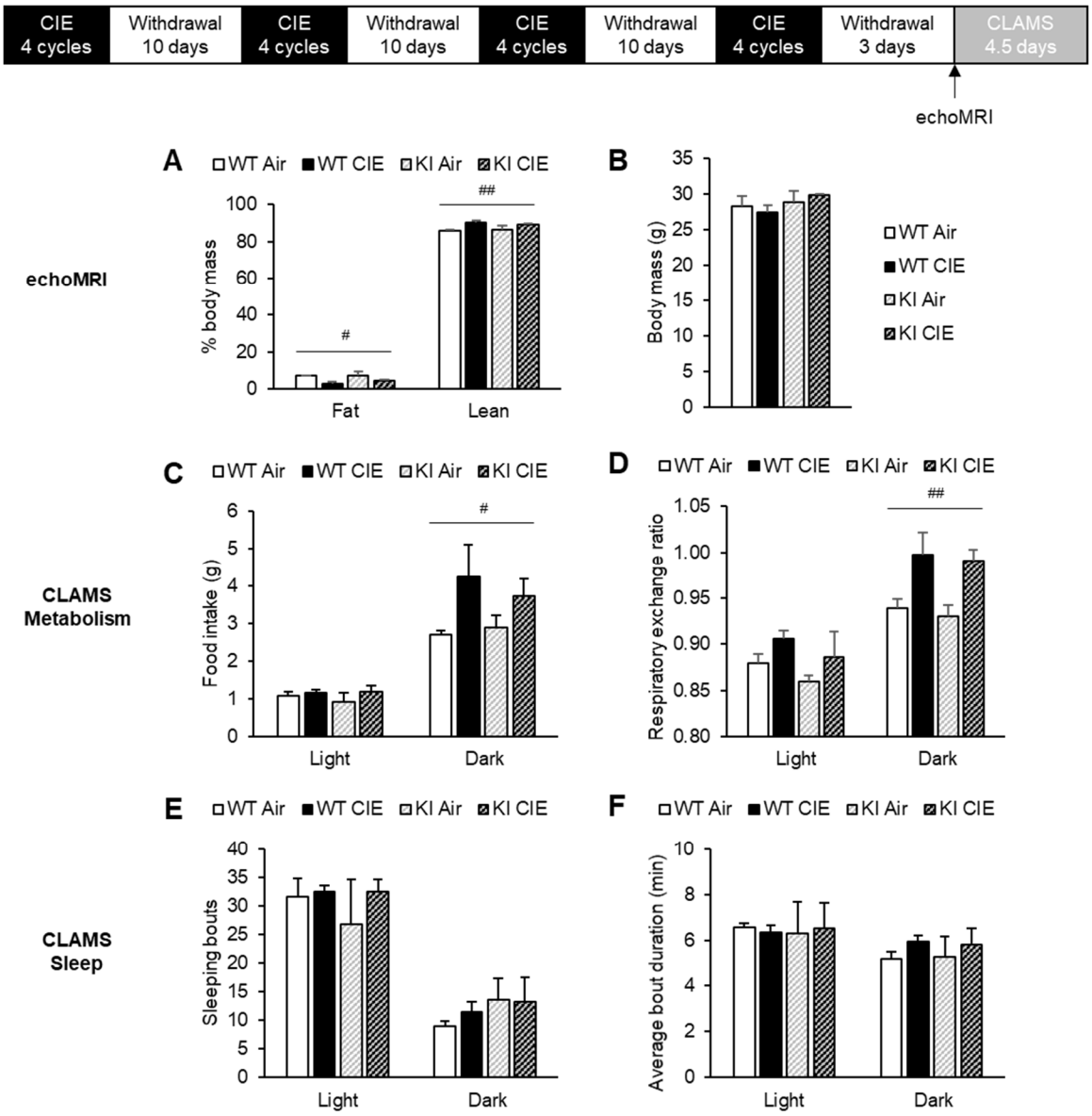

Figure 5. The BK α K361N mutation does not influence the metabolic effects of chronic intermittent ethanol (CIE) exposure

BK α K361N WT (n=8) and KI (n=7) mice were exposed to air or chronic intermittent ethanol (CIE) vapor inhalation. Body composition was determined 3 days into withdrawal (**A-B**). Food intake (**C**), respiratory exchange ratio (**D**), sleep bout number (**E**) and duration (**F**) were then recorded in metabolic chambers during 4.5 days. Main effect of vapor: #, $p<0.05$; ##, $p<0.01$. None of the measures was significantly affected by genotype. Main effects of circadian phase are not shown (see *Table 1* for details). Data are shown as mean ± s.e.m.

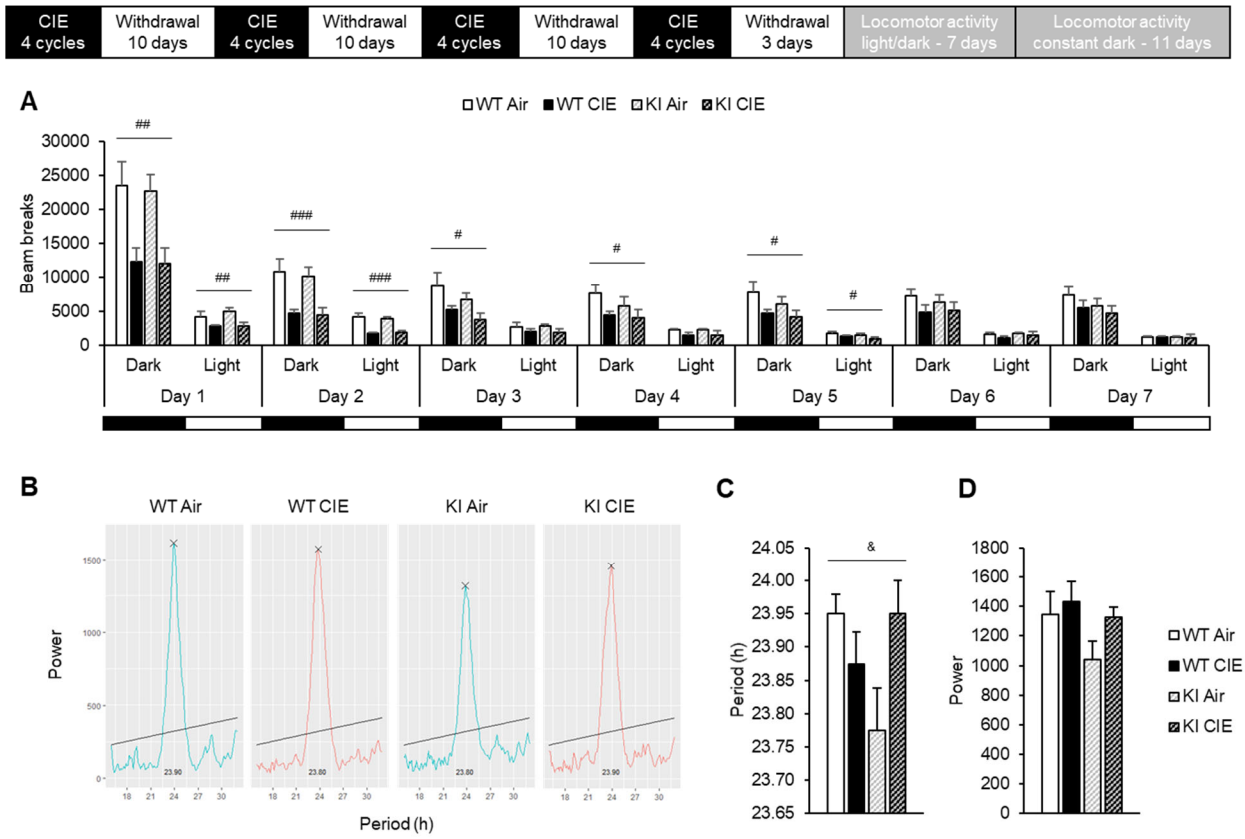

Figure 6. The BK α K361N mutation does not influence activity changes induced by chronic intermittent ethanol (CIE) exposure

BK α K361N WT (n=8) and KI (n=8) mice were exposed to air or chronic intermittent ethanol (CIE) vapor inhalation. Locomotor activity was recorded starting 3 days into withdrawal (**A**). CIE significantly reduced ambulation up to withdrawal day 8 ($^{\#}$, $p<0.05$; $^{\#\#}$, $p<0.01$; $^{\#\#\#}$, $p<0.001$). After 7 days, mice were switched to constant darkness and periodogram analysis (representative plots shown in **B**) was used to determine the free-running circadian period length (**C**) and relative power (**D**). There was a significant genotype x vapor interaction on the period ($^{\&}$, $p<0.05$) but none of the pairwise comparisons reached significance. Data are shown as mean ± s.e.m.

	Genotype	Vapor	Genotype x Vapor	Phase	Phase x Genotype	Phase x Vapor	Phase x Genotype x Vapor
Food intake	$F_{1,10}$=0.25 p=0.63	$F_{1,10}$=9.3 p=0.012	$F_{1,10}$=0.37 p=0.56	$F_{1,10}$=89.7 P<0.0001	$F_{1,10}$=0.02 p=0.88	$F_{1,10}$=4.4 p=0.063	$F_{1,10}$=0.84 p=0.38
Respiratory exchange ratio	$F_{1,10}$=0.98 p=0.34	$F_{1,10}$=9.4 p=0.012	$F_{1,10}$<0.01 p=0.96	$F_{1,10}$=234 P<0.0001	$F_{1,10}$=1.4 p=0.26	$F_{1,10}$=9.5 p=0.011	$F_{1,10}$<0.01 p=0.93
Sleeping bouts	$F_{1,11}$=0.02 p=0.90	$F_{1,11}$=0.4 p=0.54	$F_{1,11}$=0.02 p=0.90	$F_{1,11}$=81.1 P<0.0001	$F_{1,11}$=1.8 p=0.20	$F_{1,11}$=0.3 p=0.60	$F_{1,11}$=0.8 p=0.39
Average sleep bout duration	$F_{1,11}$<0.01 p=0.97	$F_{1,11}$=0.2 p=0.66	$F_{1,11}$<0.01 p=0.94	$F_{1,11}$=17.9 P=0.0014	$F_{1,11}$<0.01 p=0.97	$F_{1,11}$=2.2 p=0.17	$F_{1,11}$=0.7 p=0.41

Table 1. RM-ANOVAs were conducted to analyze the influence of genotype and alcohol vapor exposure on metabolic and sleep parameters during the light and dark phases. Data were collected over 4 consecutive periods of 24 h, starting 3 days after the last vapor exposure. Corresponding data are plotted in Figure 5.